Eur Radiol (2018) 28:1257–1266
DOI 10.1007/s00330-017-5034-2

CARDIAC

Myocardial deformation assessed by longitudinal strain: Chamber specific normative data for CMR-feature tracking from the German competence network for congenital heart defects

Quanliang Shang[1,2] · Shivani Patel[1] · Michael Steinmetz[3] · Andreas Schuster[4] · David A. Danford[1] · Philipp Beerbaum[5] · Samir Sarikouch[5] · Shelby Kutty[1]

Received: 24 August 2016 / Revised: 9 August 2017 / Accepted: 14 August 2017 / Published online: 5 September 2017

Abstract

Purpose Left ventricular two-dimensional global longitudinal strain (LS) is superior to ejection fraction (EF) as predictor of outcome. We provide reference data for atrial and ventricular global LS during childhood and adolescence by CMR feature tracking (FT).

Methods We prospectively enrolled 115 healthy subjects (56 male, mean age 12.4 ± 4.1 years) at a single institution. CMR consisted of standard two-dimensional steady-state free-precession acquisitions. CMR-FT was performed on ventricular horizontal long-axis images for derivation of right and left atrial (RA, LA) and right and left ventricular (RV, LV) peak global LS. End-diastolic volumes (EDVs) and EF were measured. Correlations were explored for LS with age, EDV and EF of each chamber.

Results Mean±SD of LS (%) for RA, RV, LA and LV were 26.56±10.2, -17.96±5.4, 26.45±10.6 and -17.47±5, respectively. There was a positive correlation of LS in LA, LV, RA and RV with corresponding EF (all P<0.05); correlations with age were weak. Gender-wise differences were not significant for atrial and ventricular LS, strain rate and displacement. Inter- and intra-observer comparisons showed moderate agreements.

Conclusions Chamber-specific nomograms for paediatric atrial and ventricular LS are provided to serve as clinical reference, and to facilitate CMR-based deformation research.

Key Points

- *No normative data exist for CMR-derived global longitudinal strain in the young.*
- *This prospective study provides reference data for atrial and ventricular longitudinal strain.*
- *The data will serve as reference for CMR-based clinical and research use.*

Keywords Paediatric cardiology · Cardiovascular magnetic resonance · Feature tracking · Strain · Cardiac deformation

Samir Sarikouch and Shelby Kutty contributed equally to this work.

✉ Shelby Kutty
skutty@unmc.edu

[1] Division of Pediatric Cardiology, University of Nebraska College of Medicine, Children's Hospital and Medical Center, Omaha, NE, USA

[2] Department of Radiology, Second Xiangya Hospital, Central South University , Changsha, Hunan Province, China

[3] Department of Paediatric Cardiology, Georg-August-University and German Centre for Cardiovascular Research (DZHK, Partner Site), Göttingen, Germany

[4] Department of Cardiology and Pulmonology, Georg-August-University and German Centre for Cardiovascular Research (DZHK, Partner Site), Göttingen, Germany

[5] Hanover Medical School, Hanover, Germany

Abbreviations

2D-STE	Two-dimensional speckle tracking echocardiography
BSA	Body surface area
CHD	Congenital heart disease
CMR-FT	Cardiac magnetic resonance-feature tracking
EDVi	End-diastolic volume indexed
EF	Ejection fraction
GCS	Global circumferential strain
LA	Left atrium
LD	Longitudinal displacement
LS	Longitudinal strain

LSR	Longitudinal strain rate
LV	Left ventricle
RA	Right atrium
RV	Right ventricle
SD	Standard deviation

Introduction

Two-dimensional longitudinal strain (LS) is a quantitative measurement of global long axis function in any cardiac chamber. Observational studies of left ventricular (LV) function in adults suggest that global LS correlates with ejection fraction (EF), and is superior to EF as a predictor of outcome [1]. Atrial function is also a key component of cardiac function, and a prognostic indicator in heart failure, myocardial infarction and atrial fibrillation [2–5]. Cardiovascular magnetic resonance (CMR) imaging with its ability to reconstruct three-dimensionally and with unlimited windows as compared to transthoracic echocardiography can provide reproducible quantitative data on cardiac chamber function [6, 7]. CMR is therefore increasingly used in children, adolescents and adults with congenital heart disease (CHD) for evaluation of ventricular function and extracardiac thoracic vascular anatomy [7]. CMR has also been shown to be accurate for analysis of atrial size and function [8–11].

Strain is the fractional change (%) in the length of a myocardial segment and strain rate is the rate of change (sec^{-1}) in strain. Strain reflects the *relative change in distance* between points of tissue along the border, characterising the deformation properties of the myocardium [12]. The terms 'global longitudinal strain' (GLS) or 'global circumferential strain' (GCS) refers to the average longitudinal or circumferential component of strain in the entire myocardium, which can be approximated by the averaged segmental strain components in individual myocardial wall segments. Depending on spatial resolution, selective analysis of layer-specific (epicardial, midwall and endocardial) strain and strain rate may also be possible.

CMR-based feature tracking (CMR-FT) is a quantitative method for assessment of cardiac mechanics that can be applied to cine images, allowing derivation of myocardial deformation using a semi-automatic tracking algorithm. In principle, CMR-FT is based on optical flow technology [13]. FT analyses tissue movement by tracking intramyocardial features detected between the epicardial and endocardial myocardial tissue boundaries and integrating the changes; the geometric shift of each feature denotes tissue motion [13, 14]. The features tracked are found by methods of maximum likelihood in two regions of interest between two frames. The technique has been validated against myocardial tagging for the LV [15], and used to identify LS abnormalities that correlated with myocardial scarring [16]. We and others have utilised LS by CMR-FT for characterisation of myocardial function in CHD, including coarctation of the aorta [17], single ventricle [18] and repaired tetralogy of Fallot [19].

Normative data for LS and strain rate by CMR-FT has recently been published for ventricular function in adults [20]. Besides ventricular LS and strain rate, CMR-FT applications to derive atrial function are evolving in adults [21]. In the paediatric population, CMR-FT analyses have the potential for functional evaluation of several forms of CHD. Paediatric application of LS by CMR-FT has been limited thus far, in part due to the absence of chamber-specific reference data. The aim of the present study was to obtain CMR-FT reference data for atrial and ventricular LS and strain rate during childhood and adolescence. We also hypothesised that there could be sex-differences in the parameters measured, as recently demonstrated for atrial and ventricular volumetry in this study cohort [7].

Materials and methods

Study population and design

The study group consisted of 115 prospectively enrolled children and adolescents of Caucasian origin, of whom 59 were female and 56 male. All subjects were examined at a single institution. This sample size was based on prior studies done by Bellenger et al., who calculated a minimal sample size of 10–15 subjects to detect clinically relevant changes in ventricular volumes, function and mass with CMR imaging [22]. We also took into consideration work from Grothues et al., who calculated sample sizes of ten and seven subjects, respectively, to detect a 10-ml change in end-diastolic and end-systolic volume, yielding a power of 90 % and an alpha- error of 0.05, with even fewer sample sizes for healthy controls [23]. Thus, with our initial aim of studying different age groups, a sample size of 115 was used.

The study participants were healthy volunteers from family and friends of hospital employees. All scans were performed in awake, non-sedated and co-operative children. All subjects were in sinus rhythm and had no acquired or CHD or any chronic illnesses, and did not participate in any competitive sports activities. Scans were performed exclusively for research purpose with no additional examination of any other organ. The local institutional ethics committee approved the study, and informed written consent was obtained from the subject's parents or legal guardians.

Cardiac magnetic resonance imaging technique

All subjects co-operated during the study and there was no use of sedation or anaesthesia for any subject. The children were placed supine onto the examination table and had vector electrocardiogram leads, an abdominal belt for detection of respiratory motion and a five-element cardiac receive coil attached.

All examinations were performed on a 1.5-Tesla (T) whole body MR scanner (Philips Medical Systems, Best, The Netherlands; Intera, R11, maximum gradient performance 30 mT/m, slew rate 150 mT/m/ms). The body coil for signal transmission and a five-element cardiac phased-array coil were used for signal acquisition. A VCG-gated balanced gradient-echo sequence (SSFP) was applied to cover the whole heart, yielding long axis (four-chamber) images, and a stack of 25–35 axial slices with 1–2 slices per breath hold. The protocol consisted of SSFP cine for axial volumetry, four-chamber view and phase contrast flow in the aorta and pulmonary artery. Further typically applied sequence parameters were no gap, repetition time/echo time/flip angle (TR/TE/flip angle) =2.8 ms/1.4 ms/60° , acquisition matrix =160×168, number of averages =1, SENSE-reduction factor of 2 (phase-encode), 5–13 *k*-space lines per phase corresponding to a gating width of 14–36 ms with an acquisition resolution of 2.0–2.5 ×1.5–1.8 mm. Depending on the patient's heart rate and physical constitution, 25–35 phases (no heart phase interpolation) were acquired aiming for a temporal resolution of 25–30 ms. A 5-mm slice thickness was used in children < 30 kg, whereas a 6-mm slice thickness was used for children > 30 kg. No angiographies were performed. The procedure followed the standardised MR imaging protocol of the German Competence Network for Congenital Heart Defects [7, 24].

CMR feature tracking

CMR cine images were analysed offline by a single observer (QS) with 2 years' experience in CMR-FT using commercially available software (2D cardiac performance analysis-MR 1.2.3.13, TomTec Imaging Systems, Unterschleissheim, Germany). Semi-automatic atrial and ventricular volumetric analysis was performed. Horizontal long axis was used for CMR-FT analysis as described elsewhere [17, 21] (Fig. 1). Atrial and ventricular longitudinal strain, strain rate and displacement were derived [17, 21, 25]. After placing points along the atrial and ventricular endocardium in a single frame, endocardial contours were manually drawn by one observer in a four-chamber view, composed of six segments. This was followed by semi-automated feature tracking by the software. Manual corrections were required in order to achieve good quality tracking. Every attempt was made to exclude the pulmonary veins, superior vena cava and suprahepatic inferior vena cava at the junction to the right atrium from atrial tracking. The atrial septum and the atrial walls were carefully reviewed for correct segmentation and manual changes performed as needed. FT computes and displays systolic and diastolic velocities, displacement, strain and times to peak for these parameters from the tracked endocardial contour by advanced analyses. The integration used to calculate displacement and strain often results in a baseline shift, for which the software automatically applies a correction (drift compensation). Because displacement, strain and strain rate are cyclic processes with no defined beginning or end, the position of a 'baseline' for tracking initiation is arbitrary [12]. The software provided segmental and average values for the measured parameters. Atrial volumes were measured from the images using a single-plane Simpson method. The interobserver and intra-observer variability was determined in 25 randomly selected healthy children by a second experienced observer (3 years of experience in CMR-FT).

Statistical analysis

All data are presented as means ± standard deviations or medians and ranges. Descriptive statistical analysis was performed for all relevant data after assessment for normality. Statistical comparisons were performed with a two-tailed unpaired Student's t-test. The relationships of data were assessed using Pearson's correlation coefficient. The Bland-Altman method was used to determine intra and interobserver variability. A p <0.05 was considered statistically significant. Statistical analysis was performed with the SPSS version 17.0.2 software package (IBM SPSS Inc., Chicago, IL, USA) and Excel 10.0 software package for Windows.

Results

Baseline demographics

A total of 115 healthy subjects participated in the study. Image quality in all studies was excellent and no images were excluded from evaluation. Demographic data and indices of global RA, RV, LA and LV function in all subjects are summarised in Table 1. It was feasible to derive deformation indices for all subjects using CMR-FT. The RVLS and LVLS were normally distributed. The mean±SD for LALS was 26.5 ±10.6 % and LVLS was -17.5±5 %. For RALS, the mean±SD value was 26.6±10.2 %, and for RVLS the mean±SD was -18 ±5.4%. The mean±SD of RA LSR, RV LSR, LA LSR and LV LSR were 1.3±0.6, -1.25±0.5, -1.52±1 and -1.19±0.4, respectively.

Gender-wise differences

Gender differences for subject age, atrial and ventricular LS, longitudinal strain rate (LSR) and longitudinal displacement (LD) were not significant (Table 2). Age-wise comparison of parameters are shown in Table 3, with age groups assigned similar to previous studies [40].

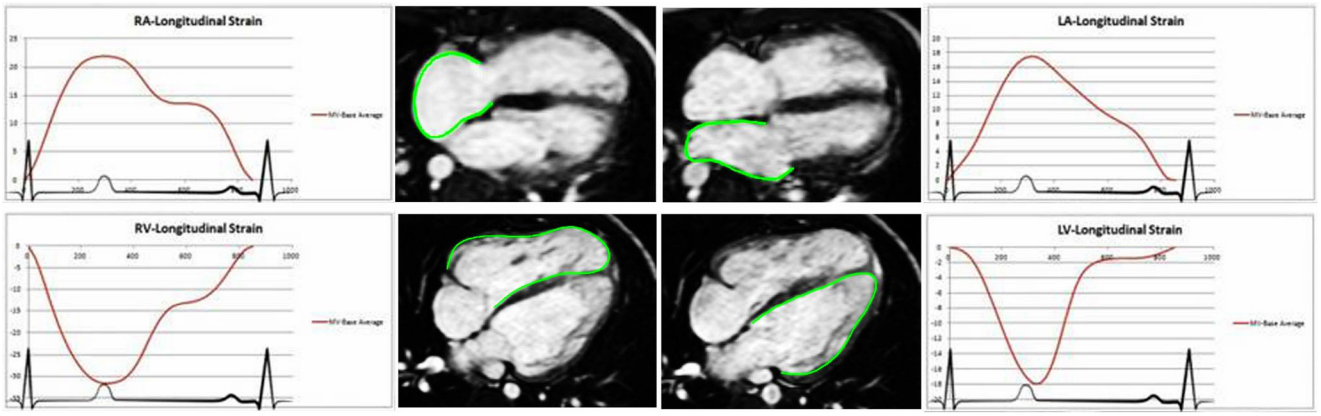

Fig. 1 CMR-FT measurements in each chamber. Demonstration of CMR-FT for each chamber derived from the four-chamber view. *CMR-FT* cardiovascular magnetic resonance feature tracking

Relationship of LS to baseline parameters and cardiac function

Correlation analysis of LS for each chamber (RA, RV, LA and LV) with age, heart rate, end-diastolic volume (EDV) and EF for the respective chamber are presented in Table 4. Relationships of strain indices with age are demonstrated in Fig. 2. LS for the RA, RV, LA and LV correlated positively with the corresponding EF: RALS had a weak positive correlation to RAEF (r =0.21, *P*=0.024), while RVLS had a moderate correlation to RVEF (r =0.35, *P*<0.001). LALS had a weak positive correlation to LAEF (r =0.32, *P*<0.001), and LVLS correlated to LVEF (r =0.27, *P*= 0.003). These results are shown in Fig. 3. There were no significant correlations for LALS, LVLS and RALS with age or EDV of the respective chamber. Age-specific normal values were not reported because there was no significant variation with age for most of the parameters. Statistically significant correlations were seen for RVLS with age (p=0.037) and RVEDV (p=0.005).

Table 1 Baseline parameters for healthy children and adolescents

Parameters (n=115)	Mean±SD
Age (years)	12.4±4.1
BSA (m^2)	1.4±0.4
RAEDV (ml)	79.9±36.2
RAEDVi (ml/m^2)	55.6±14.1
RAEF (%)	54.8±7.8
RVEDV (ml)	114.6±42.7
RVEDVi (ml/m2)	80.7±11.9
RVEF (%)	62.2±4.4
LAEDV (ml)	64.7±26.1
LAEDVi (ml/m2)	45.4±9.5
LAEF (%)	55.0±6.0
LVEDV (ml)	115.8±44.4
LVEDVi (ml/m2)	81.4±12.9
LVEF (%)	63.9±5.6

BSA body surface area, *RA* right atrium, *EF* ejection fraction, *RV* right ventricle, *EDV* end-diastolic volume, *EDVi* end-diastolic volume indexed, *LA* left atrium, *LV* left ventricle

Interobserver and intra-observer variability

Interobserver and intra-observer variability comparison showed good agreement for atrial and ventricular volumes with high correlation coefficients for each chamber (Table 5). The interobserver and intra-observer variability and the intraclass correlation for the LS measurements were lower for all chambers, but acceptable and in line with the literature (Table 6 and Fig. 4).

Table 2 Longitudinal strain, strain rate and displacement of the atrium and ventricle in healthy girls and boys

	All n=115	Female n=59	Male n=56	*p* value (female vs. male)
Age (years)	12.4±4.1	11.8±3.8	12.9±4.2	0.1442
BSA(m^2)	1.4±0.4	1.32±0.3	1.48±0.4	0.0291
RALS (%)	26.56±10.2	26.60±11.0	26.52±9.3	0.9668
RA LSR	1.3±0.6	1.35±0.7	1.24±0.5	0.3565
RA LD	-3.22±1.9	-3.09±1.8	-3.36±2.0	0.4577
LALS (%)	26.45±10.6	27.23±11.4	25.63±11.6	0.4707
LA LSR	1.52±1.0	1.60±1.2	1.45±0.8	0.4281
LA LD	-1.86±1.3	-1.72±1.2	-2.02±1.4	0.2126
RVLS (%)	-17.96±5.4	-18.47±6.1	-17.43±4.4	0.2981
RV LSR	-1.25±0.5	-1.29±0.6	-1.21±0.5	0.3782
RV LD	4.38±1.8	4.26±1.9	4.51±1.8	0.4682
LVLS (%)	-17.47±5	-17.66±5.7	-17.26±4.2	0.6665
LV LSR	-1.19±0.4	-1.19±0.4	-1.19±0.4	0.9865
LV LD	1.51±1.3	1.36±1.2	1.66±1.5	0.2246

LA left atrium, *LD* longitudinal displacement, *LS* longitudinal strain, *LSR* longitudinal strain rate, *LV* left ventricle, *RA* right atrium, *RV* right ventricle

Table 3 Longitudinal strain, strain rate and displacement of the atrium and ventricle in healthy children of different age groups

Parameters	Group I (4–10 years) N=39	Group II (10–15 years) N= 41	Group III (15–20 years) N=35
RALS (%)	25.0±10.8	27.5±10.8	27.2±8.7
RA LSR	1.3±0.7	1.4±0.6	1.2±0.4
RA LD	-2.8±1.5	-3.0±1.8	-4.0±2.2
LALS (%)	26.3±11.7	27.7±10.5	25.1±9.4
LA LSR	1.7±1.2	1.6±1.0	1.2±0.7
LA LD	-1.9±1.2	-1.8±1.0	-1.8±1.7
RVLS (%)	-18.5±5.0	-17.7±5.2	-17.6±3.6
RV LSR	-1.3±0.5	-1.3±0.5	-1.1±0.5
RV LD	3.9±1.5	4.1±1.7	5.2±2.1
LVLS (%)	-17.9±4.4	-18.2±4.9	-17.4±4.4
LV LSR	-1.2±0.4	-1.2±0.4	-1.1±0.4
LV LD	1.3±1.0	1.3±1.0	1.9±1.8

LA left atrium, *LD* longitudinal displacement, *LS* longitudinal strain, *LSR* longitudinal strain rate, *LV* left ventricle, *RA* right atrium, *RV* right ventricle

Discussion

Global LS is the most widely used index of myocardial deformation in cardiac imaging literature and clinical practice. The prognostic value of LS by speckle-tracking echocardiography has been demonstrated in children and adults [26, 27]. Stanton et al. have reported incremental prognostic value and superior mortality prediction with GLS compared with EF and wall motion score index in patients referred for echocardiography [27]. Buss et al. followed 210 patients with dilated cardiomyopathy who underwent conventional CMR with subsequent CMR-FT–derived assessment of radial, circumferential, and longitudinal strain measurements during a period of 5.3 years. They found significant associations of all strain parameters with mortality. GLS was found to be an independent and superior predictor of outcome when compared with radial and circumferential strain, N-terminal of brain natriuretic peptide, EF and scar burden defined by late gadolinium enhancement [28].

Table 4 Correlation of longitudinal strain (LS) of each chamber against baseline parameters

	r	Significance
RALS vs. RAEDV	0.09	p=0.326
RALS vs. RAEF	0.21	p= 0.024*
RALS vs. Age	0.02	p= 0.833
RALS vs. HR	0.0174	p= 0.8587
LALS vs. LAEDV	0.10	p= 0.272
LALS vs. LAEF	0.32	p<0.001*
LALS vs. Age	0.01	p=0.915
LALS vs. HR	0.1267	p=0.1934
RVLS vs. RVEDV	-0.26	p=0.005
RVLS vs. RVEF	0.35	p<0.001*
RVLS vs. Age	-0.20	p=0.037
RVLS vs. HR	0.2359	p=0.0144
LVLS vs. LVEDV	-0.06	p=0.504
LVLS vs. LVEF	0.27	p=0.003*
LVLS vs. Age	-0.01	p=0.926
LVLS vs. HR	0.0956	p=0.3274

EDV end-diastolic volume, *EF* ejection fraction, *HR* heart rate, *LA* left atrium, *LD* longitudinal displacement, *LSR* longitudinal strain rate, *LV* left ventricle, *RA* right atrium, *RV* right ventricle

*Statistical significance

Displacement defines the *distance that a feature has moved* (cm) between two consecutive frames. Velocity is the *displacement per unit of time* (cm/s), which measures how fast the location of a feature changes. Displacement and velocity are vectors, having direction in addition to magnitude. Their spatial components can be examined along the x, y and z directions; or alternatively along the anatomical coordinates of the cardiac chambers (longitudinal, radial and circumferential components) for the characterisation of myocardial mechanics [12]. Similar logic applies to strain and strain rate. The important advantage of strain and strain rate over displacement is that they reflect regional function independently of translational motion.

The accuracy of any tracking algorithm is dependent on image quality. The tracking quality achieved with CMR-FT is comparable to that of two-dimensional echocardiographic speckle tracking (2D-STE) [29]. Both tools provide quantitative deformation data including displacement, velocity and strain. We and others have shown that longitudinal and circumferential strains have good reproducibility in the FT algorithm. LV GLS was shown to have superior interobserver agreement by CMR-FT, whereas GCS had the best agreement between 2D-STE and CMR-FT. Frame rates of acquired

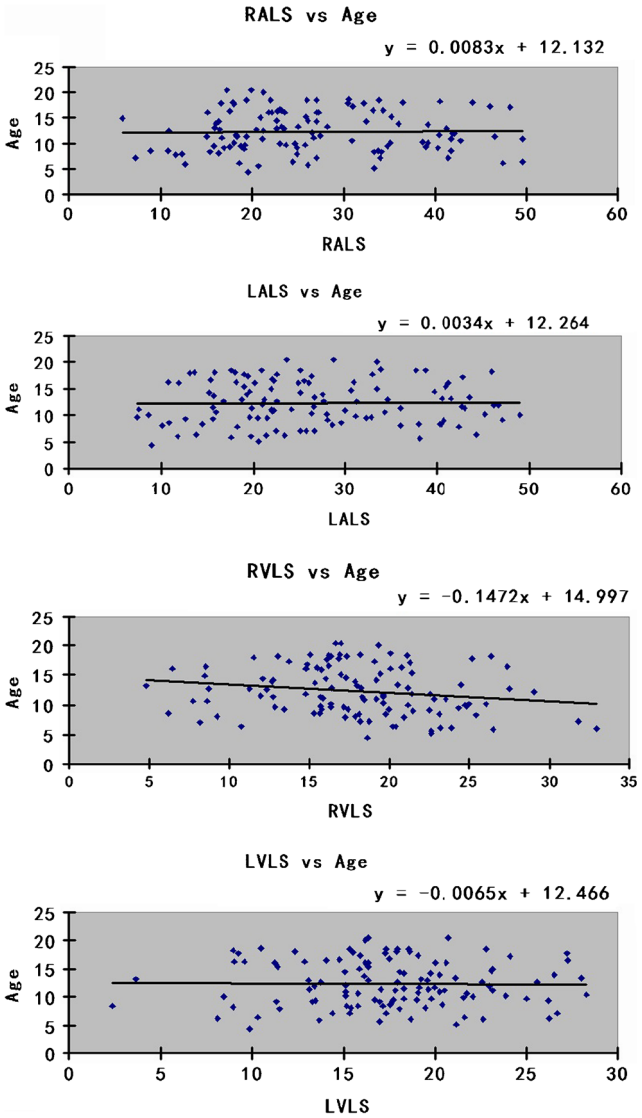

Fig. 2 Relationships of longitudinal strain with age.*LA* left atrium, *LS* longitudinal strain, *LV* left ventricle, *RA* right atrium, *RV* right ventricle

images are typically higher for 2D-STE as compared to CMR-FT. Lower frame rates in CMR-FT can result in under-sampling, whereby isovolumic phases may be affected and peak strain rate and velocity values may be reduced [30], whereas strain and displacement measurements are less affected. In other words, the lower temporal resolution of CMR images may give rise to more relative motion of a given feature in between frames, affecting the tracking results. 2D-STE has a resolution advantage; however, CMR has greater signal-to-noise ratio and thereby improved endocardial border tracking. Future studies assessing the impact of spatial and temporal resolution on the tracking accuracy of CMR-FT are important to undertake.

In the present investigation, we provide normal reference values for LS, strain rate and LD for the LA, LV, RA and RV using CMR-FT, derived from a well-characterised group of healthy children and adolescents. No significant changes were observed in global LS with increasing age. Various authors have demonstrated maturational changes in left ventricular systolic deformation indices during growth using 2D-STE [31, 32]. Andre et al. found strain and strain rates to differ between genders as well as between age groups [31]. Others have observed weak but significant influence of body size on 2D-STE-derived LS in children [33]. Variations in values depended on the vendor used, LV end-diastolic diameter and age, suggesting the importance of vendor-independent software platforms for analysing strain [34]. Marcus et al. reported increase in LV LS up to 10 years of age and remaining stable thereafter [35]. Zhang et al. found similar correlations between peak systolic strain and age, and significant but small differences for LS between age groups [36]. On the other hand, Lorch et al. [37] found weak correlations of LV LS with age, which is also in agreement with our results.

The role of the atria in children and in CHD has not been extensively studied. Several paediatric heart diseases are associated with increased ventricular stiffness or decreased compliance, which in turn may lead to elevated atrial pressure and atrial remodelling. Similar to the assessment of diastolic heart

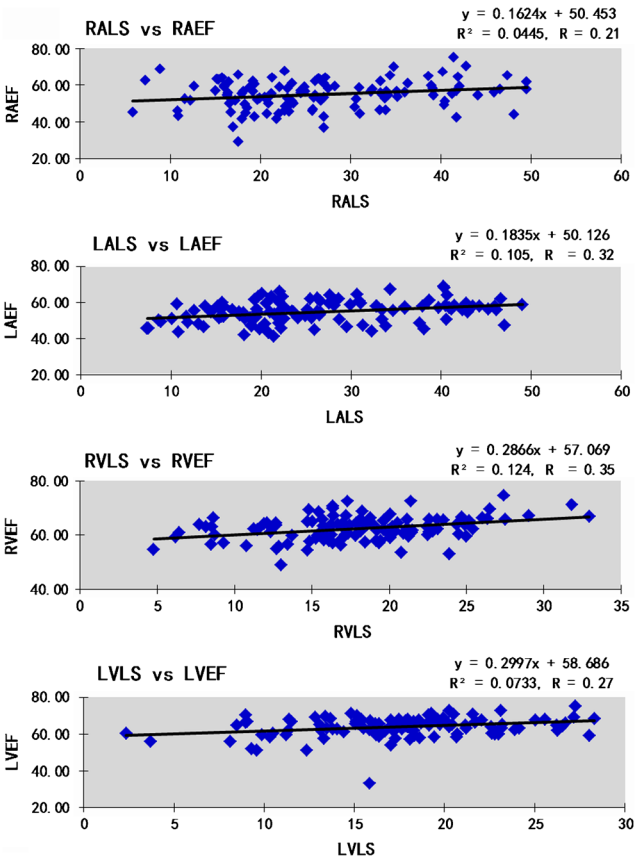

Fig. 3 Correlation of longitudinal strain (LS) and ejection fraction (EF) for each chamber. *LA* left atrium, *LV* left ventricle, *RA* right atrium, *RV* right ventricle

Table 5 Intra-observer and interobserver variability in atrial and ventricular volumes

		RAEDV	RAESV	LAEDV	LAESV	RVEDV	RVESV	LVEDV	LVESV
Intra-observer variability	Mean difference	4.7	4.1	3.3	3.5	3.1	0.5	2.6	4.9
	LOA	-8.3 to18.2	-8.5 to 17.4	-7.2 to 12.9	-7.6 to 14.3	−7.6 to 13.7	−16.0 to 16.9	−5.9 to 11.1	−8.6 to 18.5
	COV	4.5	4.3	3.4	3.6	3.5	4.8	2.6	4.2
	R	0.921	0.937	0.952	0.959	0.990	0.979	0.994	0.994
Interobserver variability	Mean difference	4.8	4.3	3.6	3.9	8.3	13.1	3.4	2.5
	LOA	-8.7 to 19.8	-8.5 to 18.7	-7.9 to 14.9	-6.8 to 15.3	−6.6 to 23.1	−13.5 to 39.8	−8.0 to 14.8	−18.0 to 22.9
	COV	5.2	4.7	3.7	4.2	6.5	10.8	3.1	5.4
	R	0.901	0.897	0.923	0.917	0.976	0.965	0.992	0.972

COV coefficient of variation, *EDV* end-diastolic volume, *ESV* end-systolic volume, *LA* left atrium, *LD* longitudinal displacement, *LOA* limits of agreement, *LS* longitudinal strain, *LSR* longitudinal strain rate, *LV* left ventricle, *R* correlation coefficient, *RA* right atrium, *RV* right ventricle

failure in adults, indices of atrial deformation derived by tissue tracking may provide insights into atrial function in paediatric and adolescent heart disease. Because parameters of myocardial deformation better reflect early myocardial dysfunction than volumetric parameters, the LS and strain rate data from this investigation could find use in the detection of preclinical disease. These data are applicable for both 1.5-T and 3.0-field strengths, as the variability in strain indices between field strengths has been shown to be negligible [14].

Our group recently showed that CMR-FT based atrial LS and strain rate discriminates between patients with impaired LV relaxation and healthy controls [21]. There is also an emerging interest in CMR-FT applications for assessment of the right heart. For example, Heermann et al. found biventricular strain analysis by CMR-FT useful to quantify wall motion abnormalities in arrhythmogenic right ventricular cardiomyopathy by permitting early detection [38]. In tetralogy of Fallot, Kempny et al. determined that right ventricular strain indices by CMR-FT related more closely with exercise tolerance than right ventricular volumetric indices [39]. Paediatric data on atrial and ventricular deformation for the left and right heart is limited, so the chamber specific values presented here could serve as clinical reference and facilitate further CMR-FT work in CHD.

It is known that the agreement between CMR-FT and myocardial tagging is not as robust for segmental LS analysis [14], and there is no validation for RV and atrial FT. The inter study reproducibility is superior for global strain as compared to segmental analysis, so global values and ranges for LS, strain rate and displacement are reported in this study. With recent literature showing the prognostic power of CMR-FT-derived biventricular strain, its clinical application for ventricular chamber quantification is likely to increase in children and adults [40]. Further studies on CMR-FT-derived circumferential strain are needed, as this parameter was more reproducible in recent studies with adults.

Limitations

As discussed in this paper, the lower temporal resolution of CMR images may give rise to more relative motion of a given feature in between frames, affecting the tracking results. Also, the feature-tracking software has not been optimally validated for the measurement of strain in non-LV chambers, which may be a limiting factor. There are no previously published data validating CMR-FT of atrial walls in direct comparison with echocardiographic speckle tracking. With the higher variability noted especially in the right ventricular longitudinal strain, reproducibility remains a current limitation, and hopefully would improve concomitantly with technical improvements in the

Table 6 Intraclass correlations (ICCs) for strain measurement for each chamber

		RALS	LALS	RVLS	LVLS
Intra-observer variability	ICC	0.747	0.599	0.959	0.982
	Lower CL 95 %	0.554	0.431	0.906	0.958
	Upper CL 95 %	0.833	0.890	0.982	0.992
Interobserver variability	ICC	0.695	0.537	0.876	0.939
	Lower CL 95 %	0.436	0.316	0.719	0.862
	Upper CL 95-%	0.870	0.867	0.945	0.973

CL confidence limit, *LA* left atrium, *LS* longitudinal strain, *LV* left ventricle, *RA* right atrium, *RV* right ventricle

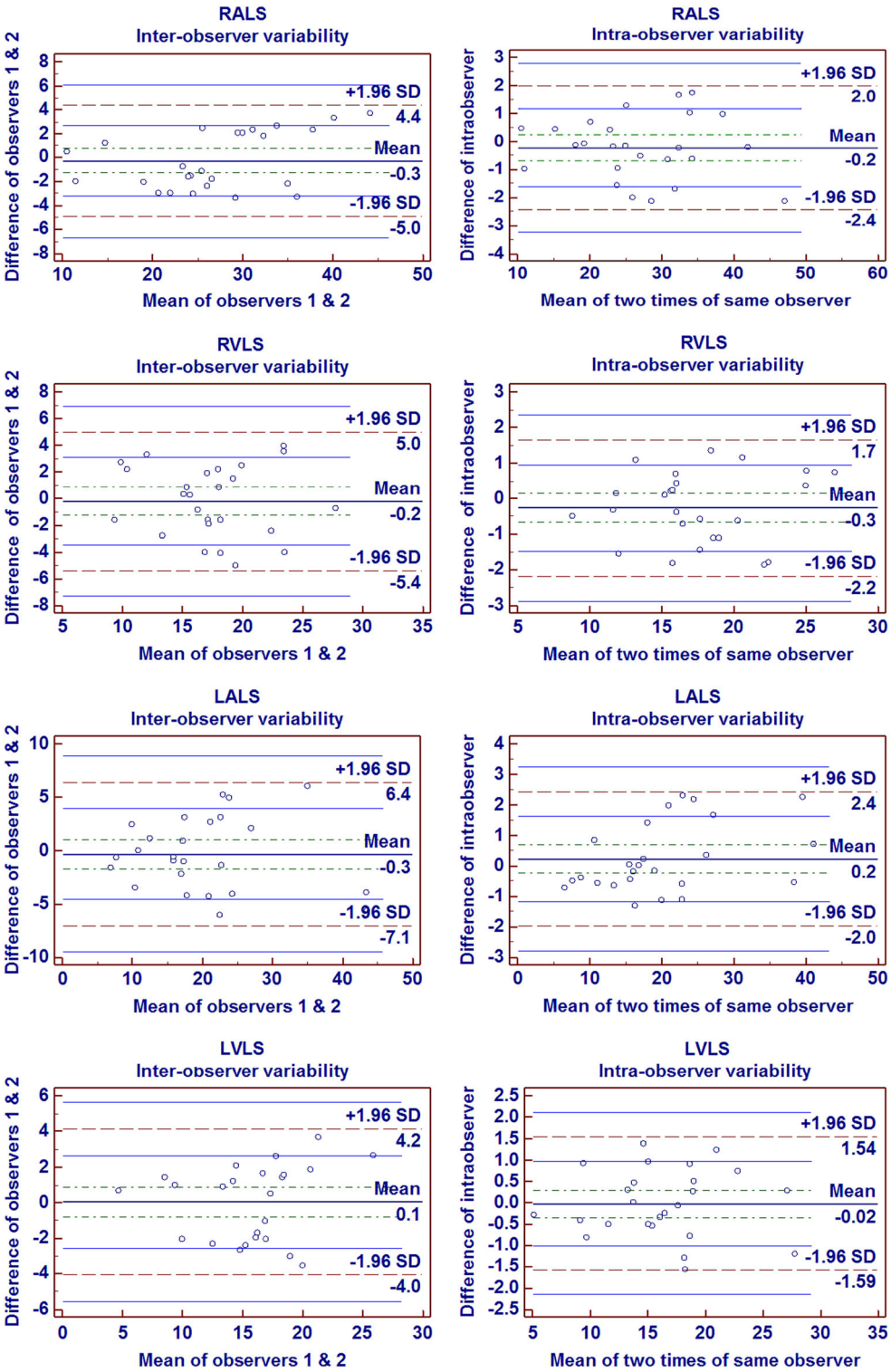

Fig. 4 Interobserver and intra-observer analysis for longitudinal strain (LS). Bland Altman plots showing the interobserver and intra-observer agreements for atrial and ventricular LS

software. Short-axis image acquisition was not part of the imaging protocol, so circumferential strain was unable to be measured in the present investigation. Correlation between strain and chamber EF was generally weak; though the reason is unclear, we speculate this may be due to measurements performed in a normal cohort with a relatively wide age range.

Recent work in a small number of healthy volunteers has demonstrated differences in strain measurements between two types of CMR-FT solutions [41]. Prospective investigations in larger numbers of patients are needed for solutions from multiple vendors to be used interchangeably. CMR-FT is limited to 2D acquisitions at the present time. In contrast to 2D

methods (STE and FTE), which cannot track motion in and out of the imaging plane, the recently developed ultrasonic 3D speckle tracking can track motion of speckles irrespective of their direction, as long as they remain within the selected scan volume. In individual patients, compared with 2D-STE, 3D-STE results in a more homogeneous spatial distribution of the measured parameters in normal ventricles. This finding is consistent with normal patterns of LV function and the fact that 3D-STE can measure all three spatial components of the myocardial displacement vector. Technical improvements including correction for through-plane motion and development of 3D CMR-FT have the potential for improving the accuracy and reproducibility of deformation measurements especially at the regional level.

Conclusions

This investigation provides chamber-specific reference values for paediatric atrial and ventricular LS, strain rate and displacement to serve as clinical reference. While there was no significant change in paediatric ventricular LS with age or gender, there were weak but significant correlations of the atrial and ventricular strain to the respective chamber EF. These data can facilitate future research in CHD based on CMR deformation. More studies correlating CMR-FT indices with clinical outcomes are needed.

Acknowledgements We thank Berthold Klas, BS, TomTec Imaging Systems, TomTec Corporation USA for technical assistance. SK receives support from the American Heart Association.

Funding This study was part of the Magnetic Resonance Imaging Project of the Competence Network for Congenital Heart Defects funded by the German Federal Ministry of Education and Research (FKZ01G10210).

Compliance with ethical standards

Guarantor The scientific guarantor of this publication is Shelby Kutty.

Conflict of interest The authors of this manuscript declare no relationships with any companies whose products or services may be related to the subject matter of the article.

Statistics and biometry David Danford kindly provided statistical advice for this manuscript.

Ethical approval Institutional Review Board approval was obtained.

Informed consent Written informed consent was obtained from all subjects (patients) in this study.

Methodology
• prospective
• cross-sectional study
• multicentre study

References

1. Ersboll M, Valeur N, Mogensen UM et al (2013) Prediction of all-cause mortality and heart failure admissions from global left ventricular longitudinal strain in patients with acute myocardial infarction and preserved left ventricular ejection fraction. J Am Coll Cardiol 61:2365–2373
2. Toh N, Kanzaki H, Nakatani S et al (2010) Left atrial volume combined with atrial pump function identifies hypertensive patients with a history of paroxysmal atrial fibrillation. Hypertension 55: 1150–1156
3. Rossi A, Temporelli PL, Quintana M et al (2009) Independent relationship of left atrial size and mortality in patients with heart failure: an individual patient meta-analysis of longitudinal data (MeRGE Heart Failure). Eur J Heart Fail 11:929–936
4. Sallach JA, Tang WH, Borowski AG et al (2009) Right atrial volume index in chronic systolic heart failure and prognosis. JACC Cardiovasc Imaging 2:527–534
5. Meris A, Amigoni M, Uno H et al (2009) Left atrial remodeling in patients with myocardial infarction complicated by heart failure, left ventricular dysfunction, or both: the VALIANT Echo study. Eur Heart J 30:56–65
6. Tandri H, Daya SK, Nasir K et al (2006) Normal reference values for the adult right ventricle by magnetic resonance imaging. Am J Cardiol 98:1660–1664
7. Sarikouch S, Peters B, Gutberlet M et al (2010a) Sex-specific pediatric percentiles for ventricular size and mass as reference values for cardiac MRI: assessment by steady-state free-precession and phase-contrast MRI flow. Circ Cardiovasc Imaging 3:65–76
8. Hudsmith LE, Petersen SE, Francis JM, Robson MD, Neubauer S (2005) Normal human left and right ventricular and left atrial dimensions using steady state free precession magnetic resonance imaging. J Cardiovasc Magn Reson 7:775–782
9. Anderson JL, Horne BD, Pennell DJ (2005) Atrial dimensions in health and left ventricular disease using cardiovascular magnetic resonance. J Cardiovasc Magn Reson 7:671–675
10. Sievers B, Kirchberg S, Franken U et al (2005) Determination of normal gender-specific left atrial dimensions by cardiovascular magnetic resonance imaging. J Cardiovasc Magn Reson 7:677–683
11. Sievers B, Addo M, Breuckmann F, Barkhausen J, Erbel R (2007) Reference right atrial function determined by steady-state free precession cardiovascular magnetic resonance. J Cardiovasc Magn Reson 9:807–814
12. Voigt JU, Pedrizzetti G, Lysyansky P et al (2015) Definitions for a common standard for 2D speckle tracking echocardiography: consensus document of the EACVI/ASE/Industry Task Force to standardize deformation imaging. Eur Heart J Cardiovasc Imaging 16: 1–11
13. Barron JL, Fleet DJ, Beauchemin SS (1994) Performance of optical flow techniques. Int J Comput Vis 12:43–77
14. Schuster A, Hor KN, Kowallick JT, Beerbaum P, Kutty S (2016) Cardiovascular Magnetic Resonance Myocardial Feature Tracking: Concepts and Clinical Applications. Circ Cardiovasc Imaging 9: e004077
15. Hor KN, Gottliebson WM, Carson C et al (2010) Comparison of magnetic resonance feature tracking for strain calculation with harmonic phase imaging analysis. JACC Cardiovasc Imaging 3:144–151
16. Maret E, Todt T, Brudin L et al (2009) Functional measurements based on feature tracking of cine magnetic resonance images identify left ventricular segments with myocardial scar. Cardiovasc Ultrasound 7:53
17. Kutty S, Rangamani S, Venkataraman J et al (2013a) Reduced global longitudinal and radial strain with normal left ventricular

ejection fraction late after effective repair of aortic coarctation: a CMR feature tracking study. Int J Card Imaging 29:141–150
18. Truong UT, Li X, Broberg CS et al (2010) Significance of mechanical alterations in single ventricle patients on twisting and circumferential strain as determined by analysis of strain from gradient cine magnetic resonance imaging sequences. Am J Cardiol 105: 1465–1469
19. Ortega M, Triedman JK, Geva T, Harrild DM (2011) Relation of left ventricular dyssynchrony measured by cardiac magnetic resonance tissue tracking in repaired tetralogy of fallot to ventricular tachycardia and death. Am J Cardiol 107:1535–1540
20. Taylor RJ, Moody WE, Umar F et al (2015) Myocardial strain measurement with feature-tracking cardiovascular magnetic resonance: normal values. Eur Heart J Cardiovasc Imaging 16:871–881
21. Kowallick JT, Kutty S, Edelmann F et al (2014) Quantification of left atrial strain and strain rate using Cardiovascular Magnetic Resonance myocardial feature tracking: a feasibility study. J Cardiovasc Magn Reson 16:60
22. Bellenger NG, Davies LC, Francis JM, Coats AJ, Pennell DJ (2000) Reduction in sample size for studies of remodeling in heart failure by the use of cardiovascular magnetic resonance. J Cardiovasc Magn Reson 2:271–278
23. Grothues F, Smith GC, Moon JC et al (2002) Comparison of interstudy reproducibility of cardiovascular magnetic resonance with two-dimensional echocardiography in normal subjects and in patients with heart failure or left ventricular hypertrophy. Am J Cardiol 90:29–34
24. Arbeitsanweisung (2008) Kardiale Magnetresonanztomographie bei angeborenen Herzfehlern. Arbeitsanweisung, German. Available via http://www.kompetenznetzahf.de/fileadmin/documents/Klinische_Studien/MRT_Arbeitsanleitung_final_MB_20080703_Web-Version.pdf
25. Kutty S, Padiyath A, Li L et al (2013b) Functional maturation of left and right atrial systolic and diastolic performance in infants, children, and adolescents. J Am Soc Echocardiogr 26:398–409
26. Poterucha JT, Kutty S, Lindquist RK, Li L, Eidem BW (2012) Changes in left ventricular longitudinal strain with anthracycline chemotherapy in adolescents precede subsequent decreased left ventricular ejection fraction. J Am Soc Echocardiogr 25:733–740
27. Stanton T, Leano R, Marwick TH (2009) Prediction of all-cause mortality from global longitudinal speckle strain: comparison with ejection fraction and wall motion scoring. Circ Cardiovasc Imaging 2:356–364
28. Buss SJ, Breuninger K, Lehrke S et al (2015) Assessment of myocardial deformation with cardiac magnetic resonance strain imaging improves risk stratification in patients with dilated cardiomyopathy. Eur Heart J Cardiovasc Imaging 16:307–315
29. Padiyath A, Gribben P, Abraham JR et al (2013) Echocardiography and cardiac magnetic resonance-based feature tracking in the assessment of myocardial mechanics in tetralogy of Fallot: an intermodality comparison. Echocardiography 30:203–210
30. Hor KN, Baumann R, Pedrizzetti G, et al (2011) Magnetic resonance derived myocardial strain assessment using feature tracking. J Vis Exp (48). https://doi.org/10.3791/2356
31. Andre F, Steen H, Matheis P et al (2015) Age- and gender-related normal left ventricular deformation assessed by cardiovascular magnetic resonance feature tracking. J Cardiovasc Magn Reson 17:25
32. Cantinotti M, Kutty S, Giordano R et al (2015) Review and status report of pediatric left ventricular systolic strain and strain rate nomograms. Heart Fail Rev 20:601–612
33. Dallaire F, Slorach C, Bradley T et al (2016) Pediatric Reference Values and Z Score Equations for Left Ventricular Systolic Strain Measured by Two-Dimensional Speckle-Tracking Echocardiography. J Am Soc Echocardiogr 29:786–793.e8
34. Jashari H, Rydberg A, Ibrahimi P et al (2015) Normal ranges of left ventricular strain in children: a meta-analysis. Cardiovasc Ultrasound 13:37
35. Marcus KA, Mavinkurve-Groothuis AM, Barends M et al (2011) Reference values for myocardial two-dimensional strain echocardiography in a healthy pediatric and young adult cohort. J Am Soc Echocardiogr 24:625–636
36. Zhang L, Gao J, Xie M et al (2013) Left ventricular three-dimensional global systolic strain by real-time three-dimensional speckle-tracking in children: feasibility, reproducibility, maturational changes, and normal ranges. J Am Soc Echocardiogr 26: 853–859
37. Lorch SM, Ludomirsky A, Singh GK (2008) Maturational and growth-related changes in left ventricular longitudinal strain and strain rate measured by two-dimensional speckle tracking echocardiography in healthy pediatric population. J Am Soc Echocardiogr 21:1207–1215
38. Heermann P, Hedderich DM, Paul M et al (2014) Biventricular myocardial strain analysis in patients with arrhythmogenic right ventricular cardiomyopathy (ARVC) using cardiovascular magnetic resonance feature tracking. J Cardiovasc Magn Reson 16:75
39. Kempny A, Fernández-Jiménez R, Orwat S et al (2012) Quantification of biventricular myocardial function using cardiac magnetic resonance feature tracking, endocardial border delineation and echocardiographic speckle tracking in patients with repaired tetralogy of fallot and healthy controls. J Cardiovasc Magn Reson 14:32
40. Yang LT, Yamashita E, Nagata Y et al (2017) Prognostic value of biventricular mechanical parameters assessed using cardiac magnetic resonance feature-tracking analysis to predict future cardiac events. J Magn Reson Imaging 45:1034–1045
41. Schuster A, Stahnke VC, Unterberg-Buchwald C et al (2015) Cardiovascular magnetic resonance feature-tracking assessment of myocardial mechanics: Intervendor agreement and considerations regarding reproducibility. Clin Radiol 70:989–998